J Nanopart Res (2011) 13:7277–7293
DOI 10.1007/s11051-011-0642-2

RESEARCH PAPER

Dynamic effects of dipolar interactions on the magnetic behavior of magnetite nanoparticles

Paolo Allia · Paola Tiberto

Received: 13 June 2011 / Accepted: 8 November 2011 / Published online: 23 November 2011

Abstract Isothermal magnetization and initial dc susceptibility of spheroidal, nearly monodisperse magnetite nanoparticles (typical diameter: 8 nm) prepared by a standard thermo-chemical route have been measured between 10 and 300 K. The samples contained magnetite nanoparticles in the form of either a dried powder (each nanoparticle being surrounded by a stable oleic acid shell as a result of the preparation procedure) or a solid dispersion in PEGDA-600 polymer; different nanoparticle (NP) concentrations in the polymer were studied. In all samples the NPs were not tightly agglomerated nor their ferromagnetic cores were directly touching. The high-temperature inverse magnetic susceptibility is always found to follow a linear law as a function of T, crossing the horizontal axis at negative temperatures ranging from 175 to about 1,000 K. The deviation from the standard superparamagnetic behavior is related to dipolar interaction among NPs; however, a careful analysis makes it hard to conclude that such a behavior originates from a dominant antiferromagnetic character of the interaction. The results are well explained considering that the studied samples are in the interacting superparamagnetic (ISP) regime. The ISP model is basically a mean field theory which allows one to straightforwardly account for the role of magnetic dipolar interaction in a NP system. The model predicts the existence of specific scaling laws for the reduced magnetization which have been confirmed in all studied samples. The interaction of each magnetic dipole moment with the local, random dipolar field produced by the other dipoles results in the presence of a large fluctuating energy term whose magnitude is comparable to the static barrier for magnetization reversal/rotation related to magnetic anisotropy. On the basis of the existing theories on thermal crossing of a barrier whose height randomly fluctuates in time it is predicted that the rate of barrier crossing is substantially driven by the rate of barrier fluctuations, which is fast (10^8–10^9 Hz) and almost independent of temperature. As a consequence, the standard picture of superparamagnetic NPs which undergo single-particle blocking by a static barrier below the blocking temperature should be substantially revised, at least in the present materials. The ISP model is perfectly matching with the view of activated magnetization rotation whose kinetics is significantly modified by barrier height fluctuations.

Keywords Magnetic nanoparticles · ISP model · Fluctuating barrier kinetics · Temperature effects · Polymer matrix

P. Allia (✉)
Politecnico di Torino, DISMIC, Corso Duca degli Abruzzi 24, 10129 Turin, Italy
e-mail: paolo.allia@polito.it

P. Tiberto
Electromagnetism Section, INRIM, Strada delle Cacce 91, 10135 Turin, Italy

Introduction

Although the interest toward fine-particle magnetism dates to more than 50 years ago, the subject of magnetic nanoparticles (NPs) has revived in the last decades in view of their increasingly pervasive applications (Gubin 2009; Sandhu et al. 2010; Wiedwald and Ziemann 2010). To date, a complete description of magnetic properties of NP materials does not exists. A striking variety of systems containing magnetic NPs can be prepared by many different techniques (Gubin 2009; Wiedwald and Ziemann 2010; Frey et al. 2009), resulting in a remarkable variety of magnetic properties which depend on NP size, shape, concentration, aggregation state. Metal or oxide NPs carrying a permanent magnetic moment can be obtained as dried nanopowders, often surrounded by some passivating shell; or, they can be dissolved in fluid hosts or embedded in solids; passivating shells and fluid/solid hosts are often diamagnetic.

A common feature of magnetic NPs is the existence of low-temperature magnetic blocking effects. In the simplest picture an assembly of free, magnetically independent NPs is characterized by a high-temperature superparamagnetic (SP) state followed at lower temperatures by a magnetically blocked state emerging as a result of single-particle blocking by magnetic anisotropy.

Of course magnetic NPs can magnetically interact in a variety of ways depending on their concentration and state of agglomeration. When magnetic NPs are not in contact and are dispersed in a non-metallic, diamagnetic medium, the dipolar interaction is the most important inter-particle energy term, and can reach a strength comparable to that of the single-particle anisotropy energy.

Isolated magnetic dipoles can be associated either to impurity atoms (Cooke et al. 1975; Roser and Corruccini 1990) or to NPs (Panissod and Drillon 2002). The temperature where magnetic dipolar interaction plays a role is now defined by $N\mu^2/k$, where μ is the magnetic moment per atom (or particle). For atomic dipolar magnets, this is in the same range as for electric dipoles, i.e., 1–10 K (Cooke et al. 1975; Roser and Corruccini 1990). However, in NP systems it can reach much higher values (Panissod and Drillon 2002), indicating that dipolar effects cannot be neglected even at high temperatures.

However, there is no commonly accepted view about the effect of dipolar energy on the directional order of magnetic moment vectors. At sufficiently low temperatures, a self sustained ordered state could emerge. As a matter of fact, different approaches provide largely different predictions in dependence of the dimensionality of the system, the arrangement of dipoles in space (whether crystalline or random) and the approximations done (Luttinger and Tisza 1946; Zhang and Widom 1995; Panissod and Drillon 2002); for 3D random systems of point dipoles the dipolar interaction generally results in an increase of the blocking temperature, while long-range magnetic ordering, either ferro- or antiferromagnetic-like, is predicted to exist above some critical volume fraction of freely rotating dipoles; on the contrary, an assembly of randomly oriented particles submitted to uniaxial anisotropy is unlikely to order (Zhang and Widom 1995).

When the temperature is high enough, dipolar systems are not expected to display self-sustained ordering; however, dipolar interactions still play a role and can be accounted for in various ways (Dormann et al. 1999; Azeggagh and Kachkachi 2007; Knobel et al. 2008; Gubin 2009). One of the existing approaches is the interacting superparamagnetic (ISP) model (Allia et al. 2001a; Knobel et al. 2008), which is particularly suitable to account for the effect of dipolar interactions on otherwise superparamagnetic NPs.

It should be noted that dipolar interactions have an inherently *dynamical* character: the dipolar field acting on a given magnetic moment is a random variable of time, so that the local dipolar energy is a fluctuating quantity. This remarkable feature has been often neglected; the ISP model was developed keeping in mind this specific aspect, but no efforts were made toward an in-depth study of the problem.

Aim of this article is to show that the dynamical aspects of dipolar interaction actually play a major role on the magnetic properties of an assembly of magnetic NPs over a broad interval of temperatures.

Specifically, the magnetic response of a NP system can be ascribed to thermally activated processes of magnetization rotation/switching which involve crossing a barrier whose height randomly fluctuates in time. The study of statistical crossing of a fluctuating barrier has received notable interest in recent years (Doering and Gadoua 1992; Bier and Astumian 1993; Pechukas and Hänggi 1994; Boguñá et al. 1998). Some theoretical results can be adapted to treat our problem, providing firmer grounds to the ISP model.

In order to apply these concepts to a practical case, a suitably simple real system of magnetic NPs is needed. To this aim, four samples containing magnetite NPs produced by a wet chemical technique were studied. The NPs were the same for all samples and were characterized by chemical homogeneity, narrow size distribution, almost spherical shape and lack of aggregation. A first sample contained a dried powder composed of individual magnetite NPs surrounded by an oleic acid shell. The other three samples contained magnetite NPs dissolved in a polymeric material at three different degrees of concentration, including a minimal one. In all cases, the magnetite NPs do not directly touch, because of the presence of an organic coating or an organic host. Exchange effects can be discarded and the role of dipolar interactions can be put in evidence.

Even for this model system, the standard interpretation (according to which the particles are in the SP regime at high temperature, and undergo single-particle blocking because of crystal anisotropy) does not hold, putting in evidence the inadequacy of the conventional views. On the contrary, the ISP theory is able to describe the magnetic properties of all samples and is instrumental in obtaining reliable values of the true magnetic moments and of the NP concentration. Moreover, the ISP model is put on firmer grounds by showing its good agreement with the proposed description of the magnetic behavior of these NPs, whose ordering kinetics is substantially determined by thermal activation over a fluctuating barrier.

Preparation and experimental methods

Fe_3O_4 NPs having mean diameter of about 8 nm were prepared by a thermo-chemical route (Sun et al. 2004). Commercial Fe(III) acetylacetonate, 1,2-hexadecanediol, oleic acid, oleylamine, benzyl ether, and *n*-hexane were used as received. Fe(acac)3 (2 mmol), 1,2-hexadecanediol (10 mmol), oleic acid (6 mmol), oleylamine (6 mmol), and benzyl ether (20 mL) were mixed and mechanically stirred under a flow of nitrogen. The mixture was heated under a nitrogen blanket to 200 °C for 2 h and then heated up to reflux (300 °C) for 1 h. After cooling down to room temperature, the solution was treated with ethanol under air. The NPs precipitated from the solution. The product was dissolved in *n*-hexane in the presence of oleic acid and oleylamine and re-precipitated with ethanol. Powders containing Fe_3O_4 NPs were obtained by drying the obtained solution.

The magnetite NP dispersion in *n*-hexane was added to the polyethylene glycol diacrylate (PEGDA-600) oligomer containing 2 wt% of radicalic photoinitiator acrylic resin in amount of 5, 10, and 90 per hundred resin. The exploited measuring unit indicates the weight percentage amount of any fluid added to a certain amount of liquid resin. The obtained mixtures were stirred reaching a uniform dispersion and the radical photoinitiator was added at a concentration of 2 wt%. The formulations were coated on silica glass substrates and the curing reaction was performed by irradiation with UV lamp with a light intensity of about 30 mW/cm^2 for 1 min under nitrogen. UV-cured transparent films about 100 μm thick containing the magnetic NPs dispersed in the diamagnetic matrix were obtained. Samples with different magnetite content are indicated in the text as PEG5, PEG10, and PEG90, respectively. The actual amount of magnetite NPs calculated by thermogravimetrical analysis after UV curing was of 0.15, 0.3, 2.7 wt% for PEG5, PEG10, PEG90 samples, respectively.

Isothermal magnetization of the dried powder was measured by a Vibrating Sample Magnetometer (VSM) under a maximum applied field of 20 kOe. The magnetization was studied in the temperature interval 10–300 K with using an liquid-He immersion cryostat.

The magnetization of the PEGx ($x = 5$, 10, 90) films was measured in the temperature interval 10–300 K by an ultra-sensitive Alternating-Gradient Field Magnetometer (AGFM) operating in the field range -18 kOe $< H <$ $+18$ kOe and equipped with a liquid-He continuous flux cryostat. In polymeric samples the magnetic signal from NPs was very low, and the diamagnetic contribution of the sample holder and polymer resin were carefully subtracted from the measured curves. In all cases, the magnetization was measured along the magnetic field direction.

Results and discussion

Details about NP structure, composition and morphology were published elsewhere (Allia et al. 2011); here a brief overview is given. SEM images were obtained on the NP powder and—with some difficulty due to

the detrimental effect of polymer's matrix—on the most concentrated polymeric sample (PEG90); no such imaging was possible on the much less concentrated PEG5 and PEG10 dispersions. An example is given in Fig. 1a, b. A SEM image of nanopowders (Fig. 1a) shows that the particles obtained by this technique are nearly spherical, being characterized by a narrow size dispersion, have a typical diameter of 8–10 nm and are surrounded by a distinguishable organic shell about 2 nm thick (light gray shades in Fig. 1a) which is responsible for the observed planar ordering and avoids direct contact of magnetic cores. These observations are in agreement with TEM images provided by other groups on similar magnetite particle systems (Guardia et al. 2007; Dutta et al. 2009). In the following, the NPs will be considered as magnetically monodisperse. Basically, they are made of magnetite; a maghemite fraction could not be excluded. The SEM image of PEG90 shows distinct and well-separated regions of higher contrast recognizable as clusters of agglomerated NPs, with average size 40 nm. This SEM image is in agreement with the outcome of magnetic data analysis, as stated in an ensuing paragraph.

This article is focused on anhysteretic magnetic properties. The measured NP size implies that all samples should be superparamagnetic at room temperature. This is never the case, although hysteresis is almost negligible at room temperature; it becomes more apparent on lowering T (Allia et al. 2011); on the basis of the measured FC/ZFC curves, blocking occurs at temperatures below 15 K for PEG5 and PEG10 (Allia et al. 2011), at about 75 K for PEG90.

An anhysteretic magnetization curve can be suitably built up by averaging the two branches of a narrow loop (Allia et al. 1999). The low-field susceptibility χ of the anhysteretic magnetization curve is identical to the average of the slopes of the ascending and descending loop branches around the respective coercive fields, as expected. In our samples, the room-temperature magnetization curves are fitted by a single Langevin function, in agreement with the SEM observation of nearly monodisperse NPs.

The temperature behavior of $\chi(T)/\chi(300\ \mathrm{K})$ is reported in Fig. 2 for all samples. The experimental curves are characterized by an increase of χ with decreasing temperature, followed by a drop of the susceptibility at low T. However, sharpness and position of the susceptibility peak strongly differ from

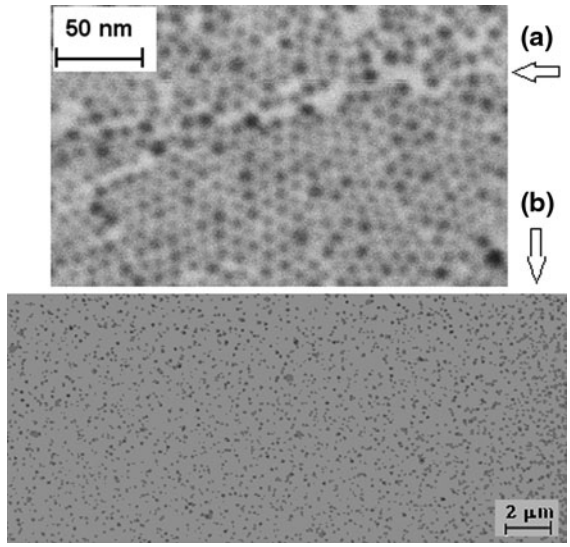

Fig. 1 **a** Contrast-enhanced Scanning Electron Micrograph of iron oxide NPs capped with oleic acid; **b** SEM image of PEGDA90 polymeric dispersion

sample to sample. The absolute value of the susceptibility (dimensionless in Gaussian units) is shown in Fig. 3, where a logarithmic scale must be used because the data differ by orders of magnitude; these values are in agreement with the different degree of dilution of the NP system in our samples.

As known, in paramagnetic materials, where the magnitude of the magnetic moments associated to magnetic ions does not change with temperature, the physically significant information can be extracted plotting $1/\chi$ as a function of temperature. In the present case, however, the magnetic moment on each NP weakly depends on temperature. In the simplest case of an ideal superparamagnetic material containing monodisperse NPs, described by a single Langevin function:

$$M = N\mu L\left(\frac{\mu H}{kT}\right) \tag{1}$$

where μ is the magnetic moment, N the number of NPs per unit volume and the saturation magnetization is $M_s = N\mu$, the function $1/\chi$ can be cast in the form:

$$\frac{1}{\chi} = 3Nk\left(\frac{T}{M_s^2}\right) \tag{2}$$

Therefore, the inverse susceptibility $1/\chi$ for a NP system should be plotted against T/M_s^2. This is done in Fig. 4 for our samples.

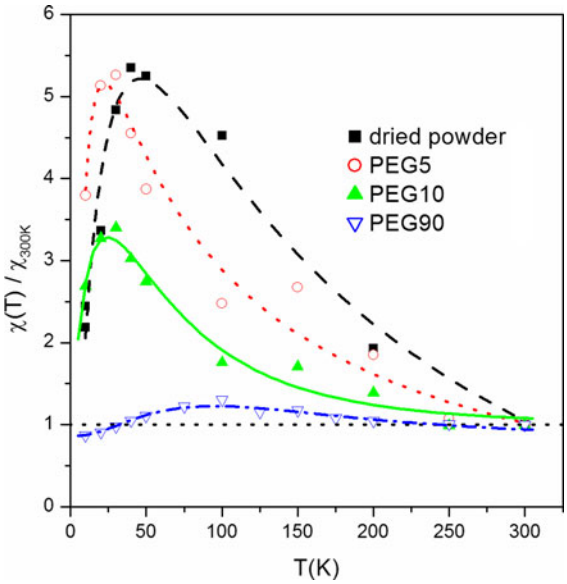

Fig. 2 Temperature behavior of the initial susceptibility of samples containing magnetite NPs. Values are normalized to χ(300 K); *lines* are guides for the eye

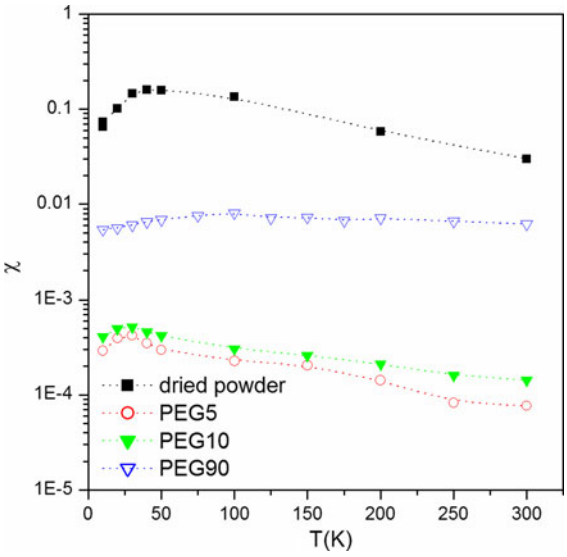

Fig. 3 Absolute initial susceptibilities of all studied samples as functions of temperature

The curves show that the ideal Curie-law corresponding for an ideal SP system is never observed, even in the most dilute polymeric sample. At high temperature, a linear behavior is indeed measured; deviations from linearity at very low temperatures can be safely ascribed to some type of particle blocking; however, the straight lines constantly intercept the

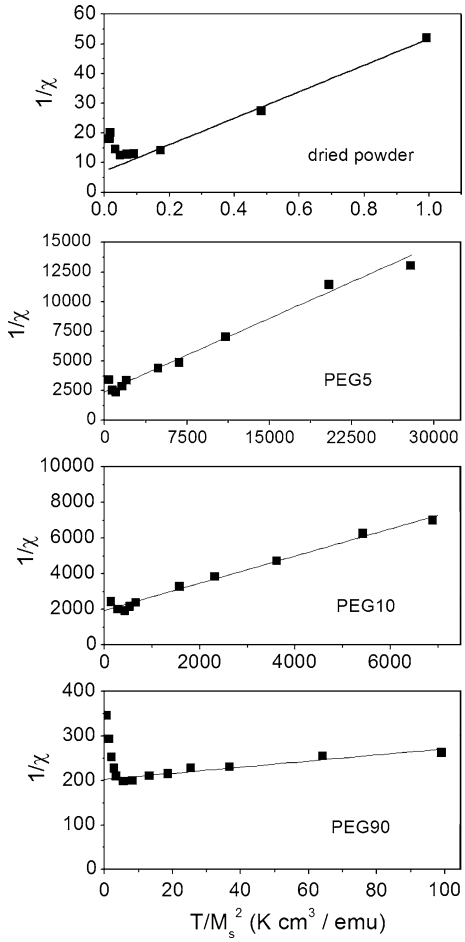

Fig. 4 Inverse susceptibility plotted as a function of the quantity T/M_s^2 for all studied samples. *Straight lines* are fits to high-temperature data

temperature axis at negative values, and are described by the law:

$$\frac{1}{\chi} = 3Nk\left(\frac{T+\theta}{M_s^2}\right) \tag{3}$$

where θ is a positive constant. A similar behavior of $1/\chi$ has been observed in a large number of different NP systems (Söffge and Schmidbauer 1981; O'Grady et al. 1983; El-Hilo et al. 1992; Gonzalez et al. 1998; Tartaj et al. 2004). Usually this circumstance is explained saying that the observed "paramagnetic Néel temperature" θ implies a predominant antiferromagnetic interaction among magnetic moments. The origin of the antiferromagnetic interaction is attributed to dipolar coupling. Some numerical models and theories support such assumption (Sauer 1940;

Luttinger and Tisza 1946; El-Hilo et al. 1992; Kechrakos and Trohidou 1998). However, here this explanation seems to be put in jeopardy when the following facts are considered:

(a) the "paramagnetic Néel' temperatures" one obtains from our fits are very high, amounting to about 175 K in PEG5, 290 K in PEG10, and 990 K in PEG90; these high values would necessarily imply the existence of an antiferromagnetically ordered phase which is instead not observed at the temperatures of interest here;
(b) the antiferromagnetic arrangement is just one of the many possible low-temperature ordered states which are expected to emerge in NP systems. In certain cases, a tendency toward ferromagnetic arrangement has been predicted also (Luttinger and Tisza 1946). In random dipole systems, frozen spin-glass states are possible also (Dormann et al. 1988; Chantrell et al. 1991); there is no general agreement about a specific role of dipolar coupling in truly favoring an antiparallel arrangement of magnetic moments.

Therefore, the presence of a negative intercept of the high-T $1/\chi$ straight line has no univocal explanation.

Such an experimental evidence can be naturally explained by the so-called ISP model (Allia et al. 2001a), which has been proposed in order to describe, in a simplified way, the temperature behavior of the magnetization curves measured in a system of isolated NPs affected by a weak but non negligible dipolar interaction. In this approach, the magnetization is thought of as described by a modified Langevin curve where the fictive temperature T^* is related to a r.m.s. dipolar energy term ε_D through the relation:

$$T^* = \frac{\varepsilon_D}{k} = \alpha \frac{\mu^2}{d^3} \tag{4}$$

where α is a positive constant of the order of unit (Vugmeister and Glinchuk 1990; Panissod and Drillon 2002), μ is the magnitude of the monodisperse magnetic moments, d is the mean interparticle distance. The ISP model prediction is:

$$\frac{1}{\chi} = 3Nk\left(\frac{T}{M_s^2}\right) + 3\alpha \tag{5}$$

whose intercept with the horizontal axis is negative. According to this view, the presence of a "Néel's temperature" is not, by itself, the hallmark of a predominantly antiferromagnetic interaction; it emerges instead as an outcome of the presence of dipolar interactions among NPs, independent of their sign. Fitting the experimental data to Eq. 5, the quantities N and α are easily obtained; using $\mu = M_s/N$ one then obtains μ and $T^* = \alpha N\mu/k$. The interacting SP is an intermediate state between the ideal SP regime and the blocked-particle regime (Allia et al. 2001a). When a ISP system is fitted to a standard Langevin curve, effective moments and an effective dipole density are obtained, according to specific transformation rules. The predictions have been verified in many systems (Allia et al. 2001a, b; Knobel et al. 2004; Franco et al. 2005; Péter et al. 2006).

Applying the ISP model to our data, one obtains the values reported in Table 1. Owing to the temperature dependence of μ, the values of this parameter and of T^* have been referred to $T = 10$ K (which corresponds to the maximum of both quantities).

Looking at the results of Table 1, one can draw the following conclusions:

(a) in the dried powder, PEG5 and PEG10 the true moments turn out to be quite similar. These systems contain the same NPs, whose mean diameter is $D = 8$ nm (Allia et al. 2011). The estimated moments are all very close to the predicted value ($1.5–2 \times 10^{-16}$ emu) obtained using $M_s \approx 500$ emu/cm^3 for the saturation magnetization of magnetite at 10 K (Allia et al. 2011). The magnetic ordering units in these samples are basically the individual NPs, as expected in PEG5 and PEG10 in reason of the great dilution in the polymeric matrix; apparently, the oleic acid shell still surrounding the NPs in the dried powder is effective in disentangling their magnetic behavior.
(b) in PEG90, the estimated moment is definitely higher than in the other samples, indicating that here the NPs are in close contact and their magnetic individuality is lost. The mean number of NP per single cluster turns out to be of the order of 20; such a conclusion is supported by the much higher NP concentration in PEG90 with respect to the two other polymeric samples. This conclusion is in agreement with direct observation (Fig. 1b).
(c) in all polymeric samples, the resulting values of NP density N and moment magnitude μ are not

Table 1 Magnetite nanoparticle concentration N, mean interparticle distance d (both referred to the entire sample), true magnetic moment μ and dipolar temperature T^* of all studied materials; magnetite nanoparticle concentration N', and mean interparticle distance d' in NP aggregates; r.m.s. dipolar energy and characteristic barrier fluctuation rate

Sample	N (cm^{-3})	d (nm)	μ (emu) ($T = 10$ K)	T^* ($T = 10$ K)	N' (cm^{-3})	d' (nm)	ε_D (erg) ($T = 10$ K)	τ_2^{-1} (Hz)
Dried powder	1.30×10^{17}	20	2.52×10^{-16}	55	1.30×10^{17}	20	1.7×10^{-14}	4.9×10^{8}
PEG5	9.94×10^{14}	100	1.67×10^{-16}	160	2.64×10^{17}	16	2.0×10^{-14}	6.6×10^{8}
PEG10	1.79×10^{15}	82	1.53×10^{-16}	200	3.97×10^{17}	14	2.7×10^{-14}	9.1×10^{8}
PEG90	1.83×10^{15}	81	4.95×10^{-15}	6,100	4.22×10^{16}	29	5.0×10^{-13}	3.1×10^{9}

sufficient to explain the measured value of T^*. This difficulty is removed thinking that N is a *mean* NP density in the material. However, many experimental data and observations with a few exceptions (Compton 2007) point to the existence of significant fluctuations in the NP density in nanocomposite polymeric materials containing magnetic NPs, either metallic or insulating, either grown within the matrix precursor or incorporated in it by mixing (Mayer 1998; Corbierre et al. 2001; Balazs et al. 2006; Sung et al. 2003; Chatterjee et al. 2009; Hall et al. 2009). These fluctuations can be related either to a specific morphology of polymeric hosts, or more generally to attractive forces among particles which act during NP growth or mixing. Concentration fluctuations can extend up to several hundreds of nanometers (Corbierre et al. 2001; Chatterjee et al. 2009) and can involve NP association or aggregation.

Our analysis indicates that in these samples also the NPs form large aggregates, where their density is much higher than the average (although the oleic acid shell coating, still present, prevents direct contact of adjacent magnetite cores), surrounded by regions of much lower NP density. In an idealized case, we assume that these aggregates are separated by regions where no particles at all are present. The NP density within each aggregate needed to account for the values of T^* is indicated as N' in Table 1, where the interparticle center-to-center distance within aggregates (d') is given too.

The following picture emerges: the dried powder is homogeneous, the NPs (bare diameter 8 nm) are at mean distance of 20 nm; recalling that the oleic acid shell is about 2 nm thick, the NP effective diameter is 12 nm; the larger distance obtained here is compatible with imperfect powder compaction; in the aggregates of PEG5 the NPs (same bare diameter) are at a mean center-to-center distance of 16 nm; this confirms that they are not in contact and can order individually; in the aggregates of PEG10 the NPs are at a mean distance of 14 nm, and a similar conclusion can be drawn; in PEG90, the magnetic units are agglomerations of about 20 NP in close contact; in turn, these agglomerates—whose size is estimated to be 20–25 nm—are still fairly well separated and can still order individually, being at a mean distance of 29 nm. This explains why T^* is so high in this material; moreover, the overall temperature behavior of the susceptibility χ approaches the standard behavior in a ferromagnet, where it is basically constant with T.

Finally, the r.m.s. dipolar energy ε_D calculated according to Eq. 4 with $\alpha \cong 1$ is reported in the last column of Table 1. For comparison, the anisotropy energy $E_0 = K_{an}V$ associated to nearly spherical, 8 nm magnetite NPs amounts to about 2.7×10^{-14} erg, $K_{an} \equiv K_1$ being in this case the cubic crystal anisotropy constant. The value $K_1 \cong 1 \times 10^5$ erg/cm^3 is appropriate in this case (Allia et al. 2011). Therefore, all estimated dipolar energies are of the same order of magnitude of, if not greater than E_0.

ISP-model scaling laws

The ISP model predicts two definite scaling regimes: a high temperature one, corresponding to $T \gg T^*$, where $m = M/M_s$ is a homogeneous function of H/T (standard SP scaling); a lower-temperature one, corresponding to $T \ll T^*$, where m becomes a homogeneous function of the ratio H/M_s (ISP scaling) (Allia et al. 2001a). This can be viewed by writing the ISP reduced magnetization for monodisperse NPs as

$$m = \frac{M}{N\mu} = L\left(\frac{\mu H}{k(T+T^*)}\right) = L\left(\frac{M_s H}{NkT + \alpha M_s^2}\right) \quad (6)$$

Either of the two scaling laws applies in dependence of which one of the addends at the denominator is predominant. Both addends are reported in Fig. 5 as functions of temperature for PEG5 and PEG90, i.e., the most dilute and the most concentrated polymeric sample. In PEG5, the NkT line crosses the αM_s^2 curve at about 130 K, so that this temperature broadly divides the temperature range in two regions, one ($T \gg 130$ K) characterized by the SP scaling law, the other ($T \ll 130$ K) characterized by the ISP scaling. This prediction is experimentally verified in Fig. 6. In PEG90, the αM_s^2 curve is constantly well above the NkT line (see Fig. 5), so that the ISP scaling is predicted to occur everywhere; Fig. 7 shows that this is indeed the case. This analysis confirms the inner coherence of the ISP model.

However, in spite of its ability to describe the magnetic behavior of a NP system over an extended temperature range, the ISP approach involves a rather unconventional treatment of the Langevin function, consisting in the introduction of a fictive temperature in the *denominator* of its argument. Usually, magnetic interactions of different types (ferromagnetic, antiferromagnetic, dipolar,…) among localized magnetic moments are depicted in the mean field approximation by adding an effective field to the *numerator* of the argument of the Brillouin or Langevin function.

Therefore, the ISP model could appear to be more a suitable representation than a real explanation of the magnetic behavior of NP systems. An attempt to establish the ISP theory on more accurate physical grounds is done in the following section.

Physical grounds of the ISP model

In monodisperse magnetic NP systems each NP carries a mesoscopic magnetic moment μ (of the order of 1×10^{-16} emu) and the mean interparticle distance d is typically of the order of 10 nm, so that the r.m.s. intensity of the dipolar field [given by $\alpha\mu/d^3$ (Zhang and Widom 1995; Panissod and Drillon 2002)] and of the associated dipolar energy ($\alpha\mu^2/d^3$) can reach substantial values. Usually the dipolar interaction is described with reference to static properties.

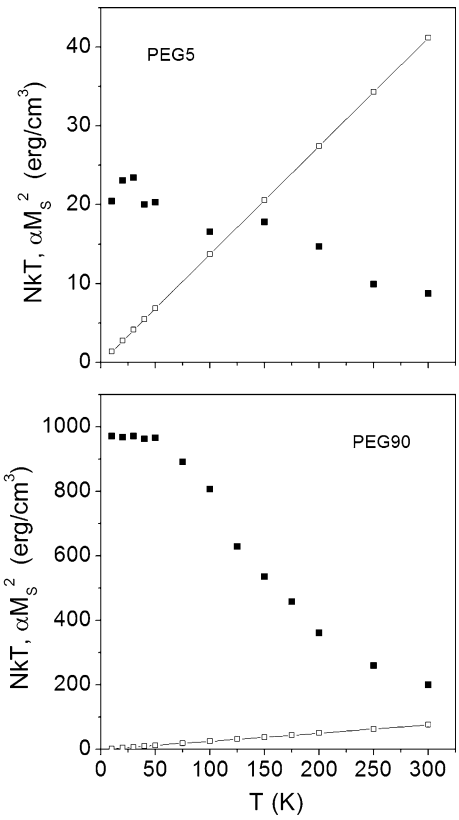

Fig. 5 Comparison between competing terms at the denominator of the modified Langevin function. See text for details

A close analogy exists between effects related to dipolar interaction in arrays of isolated electric (Vugmeister and Glinchuk 1990) and magnetic (Panissod and Drillon 2002) dipoles. However, electric dipoles are typically associated to specific impurity atoms, so that a fully quantum approach is needed and the interaction has measurable effects at very low temperatures. The temperature where electric dipolar interaction plays a role is given by the ratio Np^2/k (in Gaussian units), N being the dipole concentration, p the electric dipole moment per atom, and k the Boltzmann's constant (Fiory 1971; Vugmeister and Glinchuk 1990; Zhang and Widom 1995). Using the values of N and p appropriate to polarizable dielectrics, this temperature is in the range 1–10 K (Fiory 1971; Vugmeister and Glinchuk 1990). For electric dipoles, the simplest theories are Lorentz-field models: the real electric field acting on a given dipole is the applied field corrected by a "dipolar field" H_{loc} which acts to reduce it. For magnetic dipole systems, mean-field theories depicting a predominantly antiferromagnetic

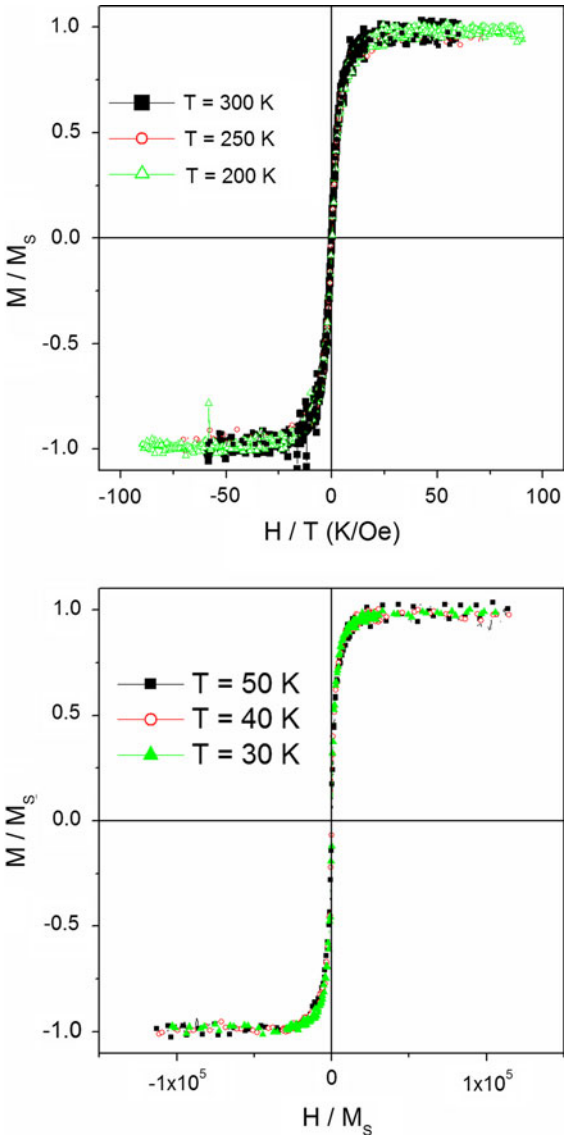

Fig. 6 Scaling laws of reduced magnetization in PEG5 sample. *Top panel*: standard SP scaling at high temperatures ($T \gg 130$ K); *bottom panel*: ISP scaling at low temperatures ($T \ll 130$ K)

coupling among moments lead to similar conclusions. However, mean-field theories do not consider the effects associated to the real distribution of point dipoles in a material. In order to gain a deeper insight on the problem, a number of numerical simulations exploiting a variety of specific techniques have been done (Panissod and Drillon 2002). Their results are however sometimes contradictory, evidencing a strong influence of the adopted starting/boundary conditions on the actual outcome of the simulation. In particular, no compelling evidence emerges that dipolar interaction in real 3D systems has a predominantly antiferromagnetic character, i.e., one which definitely favors antiparallel alignment of nearby magnetic moments. Indeed, in 3D systems of magnetic NPs a whole spectrum of site-dependent dipolar energies ranging from positive and negative is expected to exist in the material, leading to a collective state which has similarities to spin glasses and has been termed dipole super-spin glass (Morup et al. 2010). However, it should be noted that in super-spin glasses the function $1/\chi$ typically follows a Curie–Weiss law with a paramagnetic Curie temperature (positive intercept with the temperature axis) (Djurberg et al. 1997; Fiorani et al. 1999).

We point out that the dipolar field acting on a given magnetic moment, and the associated energy, are not only characterized by their magnitude; these quantities are rapidly fluctuating in time. However, such a dynamical effect is usually disregarded in virtually all approaches which are focused on equilibrium or stationary properties.

The ISP model is explicitly based on the recognition that the dynamical aspects of the dipolar interaction in a NP system should not be neglected even when equilibrium/stationary properties are addressed.

The local dipolar field $H_{\rm loc} = \alpha\mu/d^3$ can be expressed as $\alpha M_{\rm s}$, $M_{\rm s}(T)$ being the saturation magnetization at temperature T (Panissod and Drillon 2002). The field fluctuates at the characteristic rate $\tau_2^{-1} = \gamma H_{\rm loc}$, where γ is the gyromagnetic ratio. A value $\gamma \cong 1.5 \times 10^7$ Hz/Oe is appropriate to magnetic NPs (Xi et al. 2006) so that τ_2^{-1} is in the range 10^8–10^9 Hz (see Table 1). The local dipolar field entering τ_2^{-1} has been obtained using the local magnetization $N'\mu$, where N' is the NP density in a typical aggregate, as discussed before. The local magnetization differs from the average magnetization (which is the measurable quantity, and is actually measured from isothermal magnetization loops) by a constant factor only, i.e., the ratio N'/N, so that it exhibits the same temperature behavior; therefore, the fluctuation rate τ_2^{-1} is weakly dependent on temperature between 10 and 300 K.

The fluctuation rate is basically the inverse of the moment–moment (transverse) relaxation time (Slichter 1996), so it is related to the decoherence of a moment's precessional motion around the field axis, and is fairly independent of temperature. In fact, the transverse relaxation time is determined by microscopic interaction

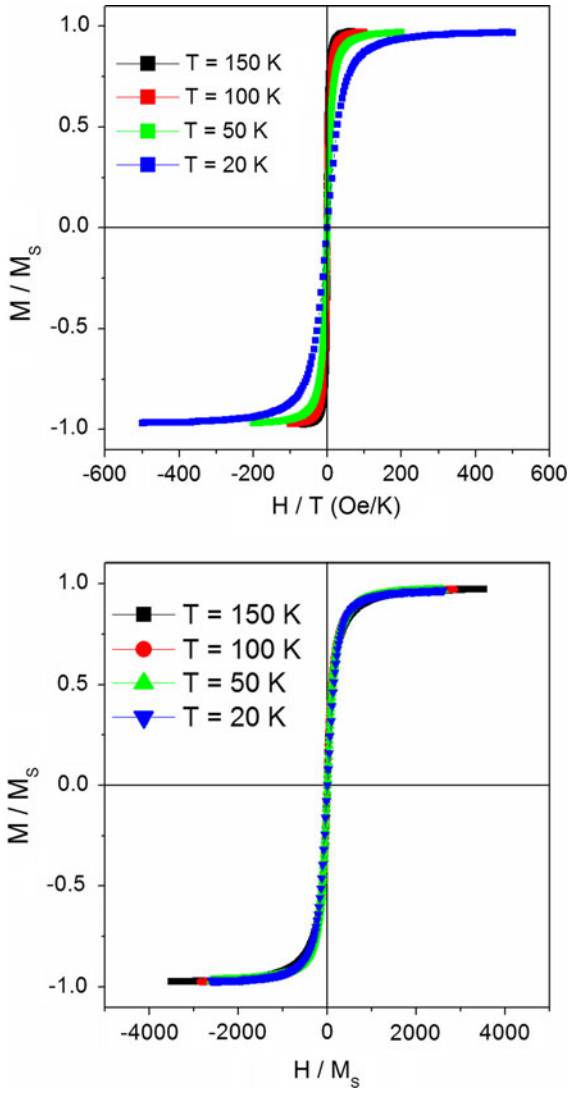

Fig. 7 Scaling laws of reduced magnetization in PEG90 sample. Standard SP scaling is not respected below 150 K (*top panel*); there, ISP scaling holds instead (*bottom panel*)

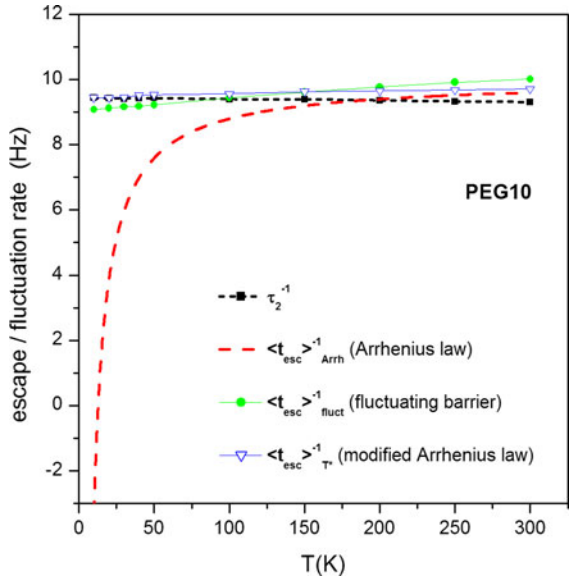

Fig. 8 Rates involved in the thermally activated process of barrier crossing for PEG10. *Filled squares* barrier fluctuation rate; *dashed line* magnetization switching rate across a static barrier according to standard Arrhenius kinetics; *filled circles* expected magnetization switching rate across a fluctuating barrier according to the DG model (see text for details); *open triangles* magnetization switching rate across a static barrier according to modified Arrhenius kinetics

processes which conserve the energy in a static field and therefore do not involve an exchange of energy between the precessing moment and the environment (Slichter 1996). In the present case $\tau_2^{-1} \approx H_{\rm loc} \approx {\rm M_S}$, so it is a weak function of T indeed. As an example, the fluctuation rate for PEG10 is reported in Fig. 8 in the interval 10–300 K (full black symbols united by a dashed line).

In magnetic NPs, thermally activated energy barrier crossing is the basic mechanism for magnetization reversal/rotation. The barrier is thought of as provided by the anisotropy energy, $E_0 = K_{\rm an}V$, $K_{\rm an}$ being the dominant anisotropy constant and V being the NP volume. The effective magnetic anisotropy can be the sum of many terms (Yanes et al. 2010). In some approaches, $K_{\rm an}$ was suitably modified to account for interparticle interactions, reducing a many-body problem to a single particle one (Dormann et al. 1999). This barrier is generally assumed to be static.

Here we explicitly consider that the barrier is given by $E = E_0 + \tilde{E}(t)$, the dipolar energy $\tilde{E}(t) = \varepsilon_{\rm D}\, f(t)$ being a random function of time whose magnitude is comparable to E_0; $f(t)$ is a Gaussian white noise process.

The problem of the activated crossing of a fluctuating classical energy barrier has received much attention in recent years, and has been addressed using different approaches (Doering and Gadoua 1992; Bier and Astumian 1993; Pechukas and Hänggi 1994; Boguñá et al. 1998). The effect of a fluctuating barrier on the escape rate of a generalized "particle" from either well of a double-well potential landscape is different in dependence of the ratio between particle escape rate and fluctuation rate. The most interesting theoretical result of the work by Doering and Gadoua

(DG) is the prediction of an interesting resonance effect (Doering and Gadoua 1992). The original DG paper provides an analytic expression for a specific case, where the barrier symmetrically fluctuates between a high positive value and a high negative value, so that the average value of the barrier is zero; numerical approaches must be used to treat more realistic cases (Doering and Gadoua 1992; Bier and Astumian 1993); an useful approximating formula has been proposed by Boguñá et al. (1998) (BPML) in the case of small amplitude of the fluctuating term with respect to E_0.

In the present case, the static anisotropy barrier E_0 is modified in amplitude by the fluctuating dipolar energy. According to Table 1, the amplitude ε_D of the fluctuating term is comparable to, and even higher than the anisotropy barrier $E_0 = 2.7 \times 10^{-14}$ erg. Therefore, the standard description of the magnetic behavior of a NP has to be substantially modified.

The escape rate of the magnetization vector across a *static* energy barrier is given by the usual Arrhenius law:

$$\langle t_{\rm esc}\rangle^{-1}_{\rm Arrh} = \tau_0^{-1} {\rm e}^{-\frac{E_0}{kT}} \tag{7}$$

whose temperature behavior is shown in Fig. 8 (dotted line). The accepted value $\tau_0^{-1} = 1 \times 10^{10}$ Hz has been used (Panissod and Drillon 2002).

At high T, the barrier fluctuates at a rate lower than the escape rate, so that the mean first-passage time (MFPT) is weakly influenced by the fluctuation of the barrier. When the temperature is decreased, however, the barrier fluctuates at a rate which rapidly becomes much higher than the Arrhenius escape rate. According to the accepted views about fluctuating-barrier crossing times, the real escape rate of the magnetization must increase, being substantially driven by the barrier fluctuation rate.

Two cases will be considered here.

(a) The fluctuating term $\tilde{E}(t)$ is comparable to or larger than the static barrier. This condition applies to the three polymeric samples. In this case, using the original DG formula is quite appropriate, also because more realistic cases exhibit a similar behavior, though being inherently not described by an analytical expression (Doering and Gadoua 1992; Boguñá et al. 1998).

In order to apply the DG approach one must transform the escape time into their dimensionless MFPT parameter $\langle\tau\rangle_{\rm DG}$ (called $\langle\tau\rangle T/L^2$ in their original paper) through:

$$\langle\tau\rangle_{\rm DG} = \frac{kT}{\xi L^2}\langle t_{\rm esc}\rangle_{\rm fluct} \tag{8}$$

where ξ is the viscous damping coefficient of the medium. This expression applies to the real overdamped motion of a mass point in space at the temperature T, L being the distance between the two potential wells separated by the barrier. In our case, the expression must be properly modified in order to be applied to the rotation of the magnetization vector. When the barrier crossing leads to the rotation of 180° of a magnetic moment, the following substitutions apply: $L \to \pi$ and $\xi \to \lambda\mu/\gamma$ where λ is the dimensionless damping constant of the Landau–Ginzburg–Gilbert (LLG) equation (Bertotti 1998). In fact, the precessing magnetic moment vector $\boldsymbol{\mu}$ is submitted to a damping torque related to the damping field $H_{\rm damp}$:

$$\begin{aligned} \gamma\mathbf{H}_{\rm damp} &= -\lambda\frac{\partial\mathbf{m}}{\partial t} \\ \tau_{\rm damp} &= -\mu\frac{\lambda}{\gamma}\frac{\partial m}{\partial t} \equiv -\xi'\frac{\partial m}{\partial t} \end{aligned} \tag{9}$$

where m is the reduced magnetization $\boldsymbol{\mu}/\mu$. The substitution $\xi \to \lambda\mu/\gamma$ proceeds by analogy with the space displacement case, where the damping force is $(-\xi \times$ velocity). As a consequence, the dimensioned escape rate is written as:

$$\langle t_{\rm esc}\rangle^{-1}_{\rm fluct} = \frac{\gamma kT}{\lambda\mu\pi^2}\langle\tau\rangle^{-1}_{\rm DG} \tag{10}$$

The DG and BPML models provide analytical expressions linking the dimensionless escape time (MFPT), i.e., $\langle\tau\rangle_{\rm DG}$, to the dimensionless fluctuation rate of the barrier (called $\langle\gamma\rangle L^2/T$ by DG and λ by BPM; called here $\tau^{-1}_{\rm barr}$ to avoid confusion of symbols). The dimensionless quantity $\tau^{-1}_{\rm barr}$ is clearly related to the dimensioned fluctuation rate τ_2^{-1} by:

$$\tau_2^{-1} = \frac{\gamma kT}{\lambda\mu\pi^2}\tau^{-1}_{\rm barr} \tag{11}$$

For a barrier fluctuation rate $\tau_2^{-1} \cong 10^9$ Hz, the common logarithm of the dimensionless barrier rate is in the range $[-1, 1.5]$; in this region the common logarithm of the dimensionless escape rate takes comparable values: the magnetization reversal is triggered by the barrier fluctuation. Taking $\lambda \cong 0.1$, which corresponds to a generally accepted value for

NP systems (Tsiantos et al. 2003; Xi et al. 2008; Hasegawa et al. 2009), it is possible to apply the DG model using our experimental data to obtain the expected value of $\langle t_{esc}\rangle^{-1}_{fluct}$ at different temperatures. The outcome of the procedure is shown in Fig. 9 for all polymeric samples. Here, the lines correspond to the DG analytical expression calculated for selected values of the E_0/kT ratio, which is the only adjustable parameter in the DG's theory (Doering and Gadoua 1992); the symbols are the values of the dimensionless escape time/rate $\langle\tau\rangle_{DG}/\langle\tau\rangle^{-1}_{DG}$ obtained from the DG formula using the experimental values of E_0/kT, $\mu(T)$ and $\tau_2^{-1} = \gamma\ \mu/d'^3$ appropriate for each measurement temperature; they are plotted in Fig. 9 as functions of the dimensionless abscissa τ_{barr} obtained from Eq. 11. Experimental data taken at different temperatures cross the family of DG lines, which are the loci of points of constant E_0/kT ratio. Note that experimental data taken at higher temperatures lie in the left-hand side of Fig. 9. Representative points for PEG90 are markedly shifted to the right because in this case the barrier height is much higher than in PEG5 and PEG10 which exhibit nearly equivalent curves (see Table 1).

The same result is better shown using dimensioned quantities for the rates, and temperature as an independent parameter, as in Fig. 8 (full circles): the escape rate remains high down to low temperatures.

Figure 8 indicates that at high temperature the escape rate predicted by the DG theory (full circles) can be larger than both the barrier fluctuation rate and the standard Arrhenius rate for a non-fluctuating barrier, considered one at a time. In fact, it is easy to show that the escape rate predicted by the original DG theory exceeds the barrier fluctuation rate, for all values of E_0/kT, when the temperature is high enough that thermally activated barrier crossing becomes the predominant effect, independent of the fact that the barrier fluctuates or not. On the other hand, the dimensioned DG escape rate can be higher than the Arrhenius rate calculated for a constant barrier height: the enhancement factor is exactly provided by barrier fluctuation. This result critically depends on the value of the Gilbert damping parameter λ. We recall that the DG model and a number of similar theories involving barrier crossing effects are valid in the overdamped regime of particle motion between adjacent energy minima; in the case of magnetic moment reversal, the overdamped regime condition corresponds to neglect the precession term with respect to the damping term in the LLG equation. In this article, a value of λ applicable to magnetic NPs and available in the literature has been used. The damping term in the LLG equation is basically $\lambda(dm/dt)$; the rate (dm/dt) corresponds to the dimensioned magnetization switching

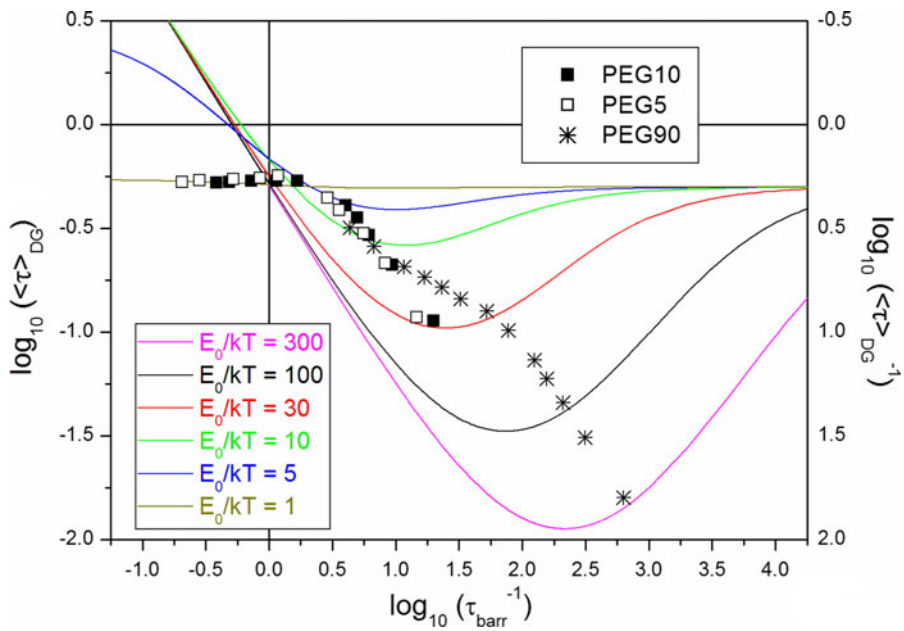

Fig. 9 Dimensionless escape rate as a function of dimensionless barrier rate. *Lines* DG theory (see text for details). *Symbols* values for all polymeric dispersions, obtained from experimental data taken at different temperatures

rate, much higher than the Larmor precession frequency at room temperature and below, over an extended temperature interval. A value of λ of the order of 0.1 is compatible with an overdamped regime. If λ is increased above 0.1, the predicted escape rate becomes much lower, as shown in Fig. 10, where the DG rates for $\lambda = 0.1$, 1, 10 are compared with the barrier fluctuation rate and the Arrhenius rate, respectively. For $\lambda = 0.1$, the DG rate is everywhere larger than the Arrhenius rate; this is no longer true for $\lambda \geq 1$, where at high temperature the kinetics of barrier crossing would be dominated by the standard Arrhenius term, the fluctuating barrier effect becoming negligible in this limit. However, this is perfectly equivalent to say that the NP system is in the true superparamagnetic regime over an extended temperature interval (e.g., above about 70 K for $\lambda = 1$). This is however never observed (see Figs. 6, 7); we can therefore assume that the choice adopted for the value of the Gilbert damping constant is basically correct.

The result depicted in Fig. 9 is in agreement with the introduction of an additional fictive temperature T^* to the denominator of the Langevin function (if a static barrier is considered, the magnetization reversal occurs at a rate corresponding to a higher temperature). In particular, the transformation operated on the Langevin function:

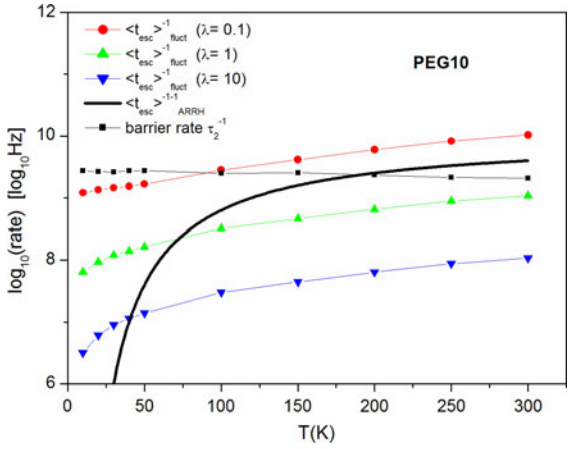

Fig. 10 Effect of Gilbert damping constant value on the magnetization switching rate across a fluctuating barrier for PEG10. *Filled squares* barrier fluctuation rate; *filled line* magnetization switching rate across a static barrier according to standard Arrhenius kinetics

$$L\left(\frac{\mu H}{kT}\right) \rightarrow L\left(\frac{\mu H}{k(T+T^*)}\right) \tag{12}$$

implies that the escape rate from the static potential well is to be modified to:

$$\langle t_{\rm esc}\rangle^{-1}_{\rm ARRH} \rightarrow \langle t_{\rm esc}\rangle^{-1}_{T^*} = \tau_0^{-1} {\rm e}^{-\frac{E_0}{k(T+T^*)}} \tag{13}$$

where the actual temperature is increased by the term T^*. This quantity is reported in Fig. 8 (open triangles) and should be compared with $\langle t_{\rm esc}\rangle^{-1}_{\rm fluct}$. In view of the many assumptions done, of the uncertainty about the parameter values and of the partial inadequacy of the DG formula to treat this specific case, the agreement could not be better. The order of magnitude of $\langle t_{\rm esc}\rangle^{-1}_{\rm fluct}$ is perfectly reproduced by $\langle t_{\rm esc}\rangle^{-1}_{T^*}$.

The expression for the T^*-corrected Arrhenius escape rate (Eq. 13) may resemble to a Vogel–Fulcher (VF) law (see, e.g., Raoult 2000); however, the denominator of the VF expression contains a term $(T - T_{\rm V})$, where the Vogel temperature $T_{\rm V}$ indicates that some critical quantity (such as viscosity or relaxation time, depending on the considered system) is diverging there. In magnetic systems, a VF law was invoked to explain the behavior of spin glasses (Souletie and Tholence 1985), where it was associated to evidence for a glass transition corresponding to cooperative freezing of magnetic moments. In those systems, the standard Arrhenius law emerges when the interaction between magnetic moments (or their concentration) is strongly decreased (Tholence 1980). The VF law was derived for interacting magnetic NP systems also (Dormann et al. 1988, 1999), at least when the interaction is weak with regard to other anisotropy energies. In all these cases, interaction among moments is viewed as instrumental in establishing a frozen magnetic configuration; in the present approach, we point out that dipolar interaction can provide an extra effect of *dynamical* disorder via the barrier fluctuation mechanism; in a sense, Eq. 13 could be referred to as representative of an "anti-VF" behavior.

The two views are in principle not contradictory, as they apply to different temperature regions of the same thermodynamic system. Magnetic interactions among moments are generally recognized as the cause of low-temperature collective blocking/freezing of either isolated spins (as in spin-glasses) or magnetic moments (in NP systems), in competition or in concurrence with single-particle blocking. Collective

blocking is heralded by critical slowing down of moment fluctuations and a simultaneous increase in the magnetic coherence length. In the case of magnetic NPs, the increase in the moment–moment correlation length gives rise to coherence domains, i.e., regions where neighboring moments fluctuate almost coherently, resulting in a strong reduction of the magnitude of the fluctuating component of each energy barrier $E = E_0 + \tilde{E}(t)$, and inhibiting the ISP effect. So, the same interaction which results in the ISP kinetics at higher temperature can be instrumental to produce a blocked state described by a Vogel–Fulcher kinetics at lower temperature. A comprehensive model of the role of dipolar interactions on the magnetic moment dynamics encompassing an extended temperature interval is however still lacking.

(b) The fluctuating term $\tilde{E}(t)$ is smaller than the static barrier. This condition applies to the dried powder sample. In this case, using the approximate BPML formula is more appropriate. Following the same steps as in point (a) above, one finds the results reported in Fig. 11. Again, the escape rate remains high down to low temperatures (even if with a more accentuated downward bending) in fairly good agreement with the modified Arrhenius law. In this case, the low-temperature magnetic response of the sample is dominated by the static barrier, so that magnetization switching is more substantially slowed down, and the ISP model begins to lose its validity below approximately 30 K. This is in agreement with the steep increase of coercivity measured in this material below 30 K (Allia et al. 2011), which indicates genuine NP blocking.

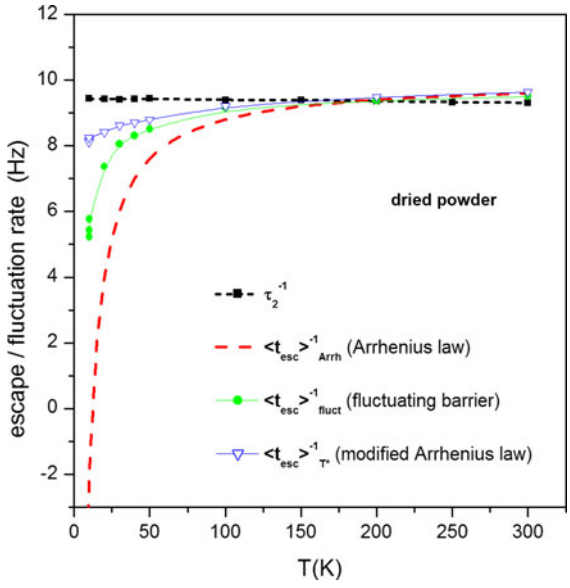

Fig. 11 Rates involved in the thermally activated process of barrier crossing for the dried powder. *Filled squares* barrier fluctuation rate; *dashed line* magnetization switching rate across a static barrier according to standard Arrhenius kinetics; *filled circles* expected magnetization switching rate across a fluctuating barrier according to the BPML model (see text for details); *open triangles* magnetization switching rate across a static barrier according to modified Arrhenius kinetics

In the light of the previous comments, the $1/\chi$ versus T plots of Fig. 4 can be coherently interpreted as follows: in all samples, the straight lines correspond to the regions of validity of the ISP approach; low-temperature deviations from the straight line imply NP blocking. However, in the dried powder, the predominant role is played by single-particle blocking because the small barrier fluctuations are unable to drastically modify the energy landscape for the reversing magnetization. In PEG5 and PEG10, single particle blocking is more effectively hindered by barrier fluctuations, which are now significantly stronger; on the other hand, *collective* blocking of magnetic moments [as predicted by the ISP model (Allia et al. 2001a)] does not occur in the examined temperature region, because the r.m.s. dipolar energy kT^* is not strong enough; as a consequence, low temperature deviations from the linear law are less apparent in both samples. In PEG90, single particle blocking is completely prevented by the huge barrier fluctuations; however, the dipolar interaction is now so strong that collective blocking of magnetic moments occurs in the examined temperature region; consequently, low-temperature data are observed to again deviate from the linear behavior.

Conclusions

The ISP model has been successfully applied to study the magnetic behavior of nearly monodisperse magnetite NPs, either prepared in the form of a dried powder, or dissolved in a polymeric matrix at different degrees of concentration. The magnetic moments which individually respond to an applied field are associated to individual NPs in the dried powder and in dilute polymeric samples; in the most concentrated sample, the analysis indicates that the individual

magnetic unit is comprised of 20 agglomerated NP on average. The temperature extension of the ISP regime vary from sample to sample according to the model's predictions.

An additional proof of the soundness of the ISP model is provided by its inherent ability to predict different scaling laws for the reduced magnetization in different temperature ranges. Scaling laws and scaling-law transformations are respected by all examined materials.

Although the ISP model is an approximate theory, its general validity has been strengthened by putting in evidence its links to the existing views about the kinetics of thermally activated crossing of a randomly fluctuating barrier. By means of a semi-quantitative treatment we have shown that introducing a fictive temperature at the denominator of the argument of the Langevin function has a deep physical meaning: in this way, the central role played by the dynamical properties of dipolar interaction is properly taken into account. The fluctuation of the dipolar field, which occurs at high rates at any finite temperature, adds to thermal effects and effectively contributes to increase the disorder of magnetic moments, in contrast to the ordering effect of an applied magnetic field. This justifies introducing an additional temperature at the denominator of the Langevin function's argument instead of an additional field at the numerator.

In our opinion, the present conclusions about the validity of the ISP model do not apply to the studied materials only; it is believed that they can be applied to many systems of magnetic NPs as well, at least well above blocking temperature. Of course the model, being aimed more to describe a general behavior than an incidental property, cannot be straightforwardly applied to any NP material in all circumstances; features such as: wide distribution of NP size; shape or aspect ratio distribution; different aggregation states, can give rise to a variety of magnetic effects not easily encompassed by a single theory. Nevertheless we believe that the ISP model may be a useful reference and a starting point for more accurate treatments.

Acknowledgments Magnetite nanoparticles were prepared by Dr. A. Suber and Dr. G. Marchegiani of ISM-CNR, Rome; nanocomposite PEGDA polymers were prepared by Dr. A. Sangermano and Dr. A. Chiolerio of the Politecnico di Torino, DISMIC.

References

Allia P, Coisson M, Knobel M, Tiberto P, Vinai F (1999) Magnetic hysteresis based on dipolar interactions in granular magnetic systems. Phys Rev B 60:12207–12218. doi:10.1103/PhysRevB.60.1220

Allia P, Coisson M, Tiberto P, Vinai F, Knobel M, Novak MA, Nunes WC (2001a) Granular Cu-Co alloys as interacting superparamagnets. Phys Rev B 64:144420-1–144420-12. doi:10.1103/PhysRevB.64.144420

Allia P, Coisson M, Tiberto P, Vinai F (2001b) Temperature behavior of anhysteretic magnetization in granular magnetic systems. J Magn Magn Mater 226–230:1904–1906. doi:10.1016/S0304-8853(00)01389-5

Allia P, Tiberto P, Coisson M, Chiolerio A, Celegato F, Vinai F, Sangermano M, Suber L, Marchegiani G (2011) Evidence for magnetic interactions among magnetite nanoparticles dispersed in photoreticulated PEGDA-600 matrix. J Nanopart Res. doi:10.1007/s11051-011-0249-7

Azeggagh M, Kachkachi H (2007) Effects of dipolar interactions on the zero-field-cooled magnetization of a nanoparticle assembly. Phys Rev B 75:174410-1–174410-7. doi:10.1103/PhysRevB.75.174410

Balazs AC, Emrick T, Russell TP (2006) Nanoparticle polymer composite: where two small worlds meet. Science 314: 1107–1110. doi:10.1126/science.1130557

Bertotti G (1998) Hysteresis in magnetism. Academic Press, San Diego, p 185

Bier M, Astumian RD (1993) Matching a diffusive and a kinetic approach for escape over a fluctuating barrier. Phys Rev Lett 7:1649–1652. doi:10.1103/PhysRevLett.71.1649

Boguñá M, Porrà JM, Masoliver J, Lindenberg K (1998) Properties of resonant activation phenomena. Phys Rev E 57:3990–4002. doi:10.1103/PhysRevE.57.3990

Chantrell RW, El-Hilo M, O'Grady K (1991) Spin-glass behavior in a fine particle system. IEEE Trans Magn 27:3570–3578. doi:10.1109/20.102929

Chatterjee U, Jewrajka SK, Guha S (2009) Dispersion of functionalized silver nanoparticles in polymer matrices: stability, characterization, and physical properties. Polym Compos 30:827–834. doi:10.1002/pc.20655

Compton J, Kranbuehl D, Martin G, Espuche E, David L (2007) In Situ Formation of a Uniform Distribution of Silver Nanoparticles in PVDF: Kinetics of Formation and Resulting Properties. Macromol Symp 247:182–189. doi:10.1002/masy.200750121

Cooke AH, Jones DA, Silva JFA, Wells MR (1975) Ferromagnetism in lithium holmium fluoride-LiHoF4. I. Magnetic measurements. J Phys C 8:4083–4088. doi:10.1088/0022-3719/8/23/021

Corbierre MK, Cameron NS, Sutton M, Mochrie SJG, Lurio LB, Ruhm A, Lennox RB (2001) Polymer-stabilized gold nanoparticles and their incorporation into polymer matrices. J Am Chem Soc 123:10411–10412. doi:10.1021/ja0166287

Djurberg C, Svedlindh P, Nordblad P, Hansen MF, Bødker F, Mørup S (1997) Dynamics of an interacting particle system: evidence of critical slowing down. Phys Rev Lett 79:5154–5157. doi:10.1103/PhysRevLett.79.5154

Doering CR, Gadoua JC (1992) Resonant activation over a fluctuating barrier. Phys Rev Lett 69:2318–2321. doi:10.1103/PhysRevLett.69.2318

Dormann JL, Bessais L, Fiorani D (1988) A dynamic study of small interacting particles: superparamagnetic model and spin-glass laws. J Phys C 21:2015–2034. doi:10.1088/0022-3719/21/10/019

Dormann JL, Fiorani D, Tronc E (1999) On the models for interparticle interactions in nanoparticle assemblies: comparison with experimental results. J Magn Magn Mater 202:251–257. doi:10.1016/S0304-8853(98)00627-1

Dutta P, Pal S, Seehra MS, Shah N, Huffman GP (2009) Size dependence of magnetic parameters and surface disorder in magnetite nanoparticles. J Appl Phys 105:07B501-1–07 B501-3. doi:10.1063/1.3055272

El-Hilo M, O'Grady K, Chantrell RW (1992) The ordering temperature in fine particle systems. J Magn Magn Mater 117:21–28. doi:10.1016/0304-8853(92)90286-W

Fiorani D, Dormann JL, Cherkaoui R, Tronc E, Lucari F, D'Orazio F, Spinu L, Nogues M, Garcia A, Testa AM (1999) Collective magnetic state in nanoparticles systems. J Magn Magn Mater 196–197:143–147. doi:10.1016/S0304-8853(98)00694-5

Fiory NT (1971) Electric dipole interactions among polar defects in alkali halides. Phys Rev B 4:614–627. doi:10.1103/PhysRevB.4.614

Franco V, Conde CF, Conde A, Kiss LF (2005) Relationship between coercivity and magnetic moment of superparamagnetic particles with dipolar interaction. Phys Rev B 72:174424-1–174424-10. doi:10.1103/PhysRevB.72.174424

Frey NA, Peng S, Cheng K, Sun S (2009) Magnetic nanoparticles: synthesis, functionalization, and applications in bioimaging and magnetic energy storage. Chem Soc Rev 38:2532–2542. doi:10.1039/B815548H

Gonzalez A, Tiberto P, Garcia-Escorial A, Paramo D, Sinnecker JP, Allia P, Hernando A (1998) Magnetic interactions in melt spun CoCu system. J Phys IV France 8:Pr2-343–Pr2-346

Guardia P, Batlle-Brugal B, Roca AG, Iglesias O, Morales MP, Serna CJ, Labarta A, Batlle X (2007) Surfactant effects in monodisperse magnetite nanoparticles of controlled size. J Magn Magn Mater 316:e756–e759. doi:10.1016/j.jmmm.2007.03.085

Gubin SP (2009) Chapter 1. Introduction. In: Gubin SP (ed) Magnetic nanoparticles. Wiley-VCH Verlag GmbH & Co. KgaA, Weinheim, pp 1–23. doi:10.1002/9783527627561

Hall LM, Anderson BJ, Zukoski CF, Schweizer KS (2009) Concentration fluctuations, local order, and the collective structure of polymer nanocomposites. Macromolecules 42:8435–8442. doi:10.1021/ma901523w

Hasegawa D, Yang H, Ogawa T, Takahashi M (2009) Challenge of ultra high frequency limit of permeability for magnetic nanoparticle assembly with organic polymer—application of superparamagnetism. J Magn Magn Mater 321:746–749. doi:10.1016/j.jmmm.2008.11.041

Kechrakos D, Trohidou KN (1998) Magnetic properties of dipolar interacting single-domain particles. Phys Rev B 58:12169–12177. doi:10.1103/PhysRevB.58.12169

Knobel M, Nunes WC, Brandl AL, Vargas JM, Socolovsky LM, Zanchet D (2004) Interaction effects in magnetic granular systems. Physica B 354:80–87. doi:10.1016/j.physb.2004.09.024

Knobel M, Nunes WC, Socolovsky LM, De Biasi E, Vargas JM, Denardin JC (2008) Superparamagnetism and other magnetic features in granular materials: a review on ideal and real systems. J Nanosci Nanotechnol 8:2836–2857. doi:10.1166/jnn.2008.017

Luttinger JM, Tisza L (1946) Theory of dipole interaction in crystals. Phys Rev 70:954–964. doi:10.1103/PhysRev.70.954

Mayer ABR (1998) Formation of noble metal nanoparticles within a polymeric matrix: nanoparticle features and overall morphologies. Mat Sci Eng C 6:155–166. doi:10.1016/S0928-4931(98)00049-6

Morup S, Fougt Hansen M, Frandsen C (2010) Magnetic interactions between nanoparticles. Beilstein J Nanotechnol 1:182–190. doi:10.3762/bjnano.1.22

O'Grady K, Bradbury A, Charles SW, Menear S, Popplewell J, Chantrell RW (1983) Curie-Weiss behavior in ferrofluids. J Magn Magn Mater 31–34:958–960. doi:10.1016/0304-8853(83)90755-2

Panissod P, Drillon M (2002) Magnetic ordering due to dipolar interaction in low dimensional materials. In: Miller JS, Drillon M (eds) Magnetism: molecules to materials, vol IV. Wiley-VCH Verlag GmbH & Co. KGaA, Weinheim, pp 232–270. ISBNs: 3-527-30429-0

Pechukas P, Hänggi P (1994) Rates of activated processes with fluctuating barriers. Phys Rev Lett 73:2772–2775. doi:10.1103/PhysRevLett.73.2772

Péter L, Rolik Z, Kiss LF, Tóth L, Weihnacht V, Schneider CM, Bakonyi I (2006) Temperature dependence of giant magnetoresistance and magnetic properties in electrodeposited Co-Cu/Cu multilayers: the role of superparamagnetic regions. Phys Rev B 73:174410-1–174410-10. doi:10.1103/PhysRevB.73.174410

Raoult J (2000) Origin of the Vogel-Fulcher-Tammann law in glass-forming materials: the a-b bifurcation. J Non-Cryst Solids 271:177–217. doi:10.1016/S0022-3093(00)00099-5

Roser MR, Corruccini LR (1990) Dipolar ferromagnetic order in a cubic system. Phys Rev Lett 65:1064–1067. doi:10.1103/PhysRevLett.65.1064

Sandhu A, Handa H, Abe M (2010) Synthesis and applications of magnetic nanoparticles for biorecognition and point of care medical diagnostics. Nanotechnology 21:442001-1–442001-44. doi:10.1088/0957-4484/21/44/442001

Sauer JA (1940) Magnetic energy constants of dipolar lattices. Phys Rev 57:142–146. doi:10.1103/PhysRev.57.142

Slichter GP (1996) Principles of magnetic resonance. Springer-Verlag, Berlin, p 33

Söffge F, Schmidbauer E (1981) AC susceptibility and static magnetic properties of AN Fe_3O_4 ferrofluid. J Magn Magn Mater 24:54–66. doi:10.1016/0304-8853(81)90100-1

Souletie J, Tholence JL (1985) Critical slowing down in spin glasses and other glasses: Fulcher versus power law. Phys Rev B 32:516–519. doi:10.1103/PhysRevB.32.516

Sun S, Zeng H, Robinson DB, Raoux S, Rice PM, Wang SX, Li G (2004) Monodisperse MFe_2O_4 (M: Fe, Co, Mn) nanoparticles. J Am Chem Soc 124:8204–8205. doi:10.1021/ja0380852

Sung LP, Scierka S, Baghai-Anaraki M, Ho DL (2003) Characterization of metal-oxide nanoparticles: synthesis and

dispersion in polymeric coatings. In: Berndt C, Fischer TE, Ovid'ko I, Skandan G, Tsakalakos T (eds) Materials Research Society proceedings, vol 740—MRS symposium I: nanomaterials for structural applications. Cambridge Journals Online, pp I5.4.1–I5.4.6. doi:10.1557/PROC-740-I5.4

Tartaj P, González-Carreño T, Bomatí-Miguel O, Serna CJ, Bonville P (2004) Magnetic behavior of superparamagnetic Fe nanocrystals confined inside submicron-sized spherical silica particles. Phys Rev B 69:094401-1–094401-8. doi:10.1103/PhysRevB.69.094401

Tholence JL (1980) On the frequency dependence of the transition temperature in spin glasses. Solid State Commun 35:113–117. doi:10.1016/0038-1098(80)90225-2

Tsiantos V, Schrefl T, Scholz W, Forster H, Suess D, Dittrich R, Fidler J (2003) Thermally activated magnetization rotation in small nanoparticles. IEEE Trans Magn 39:2507–2509. doi:10.1109/TMAG.2003.816456

Vugmeister BE, Glinchuk MD (1990) Dipole glass and ferroelectricity in random-site electric dipole systems. Rev Mod Phys 62:993–1026. doi:10.1103/RevModPhys.62.993

Wiedwald U, Ziemann P (2010) Preparation, properties and applications of magnetic nanoparticles. Beilstein J Nanotechnol 1:21–23. doi:10.3762/bjnano.1.4

Xi H, Gao KZ, Shi Y, Xue S (2006) Precessional dynamics of single-domain magnetic nanoparticles driven by small ac magnetic fields. J Phys D: Appl Phys 39:4746–4752. doi:10.1088/0022-3727/39/22/002

Xi H, Gao KZ, Xue S (2008) Reversal of single-domain magnetic nanoparticles induced by pulsed magnetic fields. J Appl Phys 103:07F502-1–07F502-3. doi:10.1063/1.2829594

Yanes R, Chubykalo-Fesenko O, Evans RFL, Chantrell RW (2010) Temperature dependence of the effective anisotropies in magnetic nanoparticles with Neel surface anisotropy. J Phys D 43:474009-1–474009-8. doi:10.1088/0022-3727/43/47/474009

Zhang H, Widom M (1995) Spontaneous magnetic order in random dipolar solids. Phys Rev B 51:8951–8957. doi:10.1103/PhysRevB.51.8951